

Figure 4: Simulated blend of two lines with  $b = 30$ ,  $\log N_{\text{HI}} = 14.1$ , separated by  $1 \text{ \AA}$ , with  $S/N = 6$ . Dotted curve: profile of the individual components. Continuous curve: single line fitted profile, with  $b = 35$  and  $\log N_{\text{HI}} = 15.1$ .

lower curve corresponds to a central flux of 0.1 where the noise level becomes comparable to the signal and lines start to saturate, in the range of  $b$  considered: lines on the right of this curve could be unresolved blends. It is clear that unsaturated lines show a tight correlation which reflects the selection effects (line-selection + non-saturation). However, the saturated lines, which are clearly identified in our spectrum, are

not uniformly distributed in the same range of  $b$  occupied by unsaturated lines. In particular, the absence of clearly single lines with  $b < 20$  and  $\log N_{\text{HI}} > 13.5$  is not due to any bias. Moreover, almost all the saturated features appear as unresolved blends and the reality of lines with  $\log N_{\text{HI}} > 14$  in our spectrum is cast in serious doubt. The same could be true for lines with  $b > 35$ .

According to this interpretation, most

of the lines which appear as saturated could be unresolved blends of unsaturated lines which should occupy the top ( $b \geq 30$  and  $\log N_{\text{HI}} \leq 14$ ) of the apparently correlated distribution, as can be seen in Figure 4 where a simulated blend of two lines with the above parameters and  $S/N = 6$  has been fitted as a single line of  $b = 35$  and  $\log N_{\text{HI}} = 15.1$ , comparable with the line of highest column density in our sample.

Thus blending plays a crucial role in the interpretation of the observations, as has been shown recently by Trèvese, Giallongo and Camurani (1992). However, increasing the signal-to-noise ratio would raise the upper curve in Figure 3 and move downwards the lower one and allow a better deblending. Thus, recognizing a possible intrinsic correlation between  $b$  and  $N_{\text{HI}}$  in the Lyman- $\alpha$  clouds is within the reach of the present ESO instrumentation.

## References

- Banase, K. et al. 1983, "MIDAS" in *Proc. of DECUS*, Zurich, 87.  
 Carswell, R.F. et al. 1987, *Ap.J.* **319**, 709.  
 Carswell, R.F. et al. 1991, *Ap.J.* **371**, 36.  
 D'Odorico, S. 1990, *The Messenger* **61**, 51.  
 Giallongo, E., Cristiani, S. and Trèvese D. 1992, *Ap.J.L.* (in press).  
 Gunn, J.E. and Peterson, B.A. 1965, *Ap.J.* **142**, 1633.  
 Lynds, C.R. 1971, *Ap.J.* **164**, L73.  
 Madau, P. 1992, *Ap.J.* **389**, L1.  
 Ostriker, J.P. and Iveuchi, S. 1983, *Ap.J.* **268**, L63.  
 Pettini, M. et al. 1990, *M.N.R.A.S.* **246**, 545.  
 Rees 1986 *M.N.R.A.S.* **218**, 25P.  
 Sargent, W.L.W. et al. 1980, *Ap.J.S.* **42**, 41.  
 Smette, A. et al. 1992, *Ap.J.* **389**, 39.  
 Steidel, C.C. and Sargent, W.L.W. 1987, *Ap.J.* **318**, L11.  
 Trèvese D., Giallongo E., and Camurani L. 1992, *Ap.J.* (in press).

# The Galaxy Population in Distant Clusters

A. BUZZONI<sup>1</sup>, M. LONGHETTI<sup>1, 2</sup>, E. MOLINARI<sup>1</sup> and G. CHINCARINI<sup>1, 2</sup>

<sup>1</sup>Osservatorio Astronomico di Brera, Milano, Italy; <sup>2</sup>Università degli Studi, Milano, Italy

## 1. Introduction

Clusters of galaxies are recognized to be the basic building blocks tracing the large-scale structure in the Universe. Thanks to the large number of coeval objects all at the same distance we get more favourable statistics allowing to explore in much better detail the

evolutionary status of the galaxy population.

Moreover, it is relevant to clarify whether or not clusters are dynamically relaxed structures and how environmental conditions constrained galaxy formation among the different morphological types. We know for instance

that ellipticals always reside in high-density regions like the core of the clusters while spirals better trace the low-density peripheral regions (Dressler 1980).

Both the dynamical and photometric questions have much in common as environment conditions might have influ-

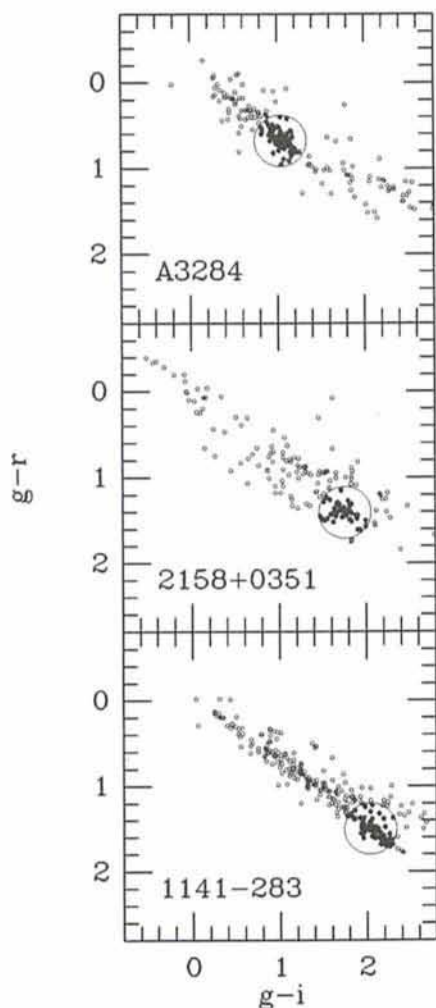


Figure 1:  $(g-r)$  vs  $(g-i)$  diagrams for the clusters A3284, 2158+0351 and 1141-283. All of the objects with complete photometry are included in the plots. The encircled clump of objects, moving to redder colours with increasing redshift, is due to the cluster elliptical galaxy population. The redshifts of the clusters are respectively 0.15, 0.45 and 0.50.

enced at the beginning the morphological and photometric properties of the galaxies. Therefore, studying cluster galaxies we get both direct clues about their evolutionary status and about that of their parent clusters.

## 2. The Blue Galaxies' Dilemma

One of the most intriguing and embarrassing problems when dealing with the cluster galaxy population is that an increasing fraction of blue galaxies (i.e. bluer than expected for a population of quiescent early-type galaxies alone) populate clusters at high redshift. This is the so-called "Butcher-Oemler effect".

Since spiral galaxies in the field are known to display similar colours, it has been first questioned that geometrical and projection effects as well as bad field subtraction could induce such a

false correlation (see for example Koo 1988 for an exhaustive discussion). In the last years however a number of observations converged detecting such a component in the population of many clusters at high redshift confirming that despite any possible complication the effect is real (Butcher and Oemler 1984b, Luppino et al. 1991, Molinari et al. 1990, Newberry et al. 1988).

Three main spectral features seem to characterize blue galaxies: (i) Most of them display emission lines (typically [OII], [OIII] and H $\beta$ ) as found for instance in the star forming spiral galaxies (Butcher and Oemler 1984a); (ii) strong Balmer lines in absorption are often detected superposed to a normal E-type continuum (E+A galaxies of Dressler and Gunn 1982, 1983), (iii) when high-resolution imaging is available (Thompson 1988) most blue galaxies seem to display a late-type morphology with signs of possible interaction.

On the basis of our present knowledge it is certainly hard to disentangle the various mechanisms leading to such profound differences in the population of late-type galaxies at early epochs. This is certainly a problem since it has to be established how such late-type galaxies can "vanish" or transform so drastically by the present time.

Alternatively, one should conclude that looking at high redshift in some way we are selecting clusters which are intrinsically different from the local sample. One reason could be that since they are mainly optically selected, the more compact ones are strongly preferred (Cappi et al. 1989). Moreover, clusters with active galaxies could be more prominent. Finally, due to k-correction effects those with a larger fraction of spirals might become more visible with increasing  $z$  (Coleman et al. 1980).

That high-redshift clusters might be somewhat different aggregates also stems from an extended analysis by Newberry et al. (1988). In particular, it appears that they display a larger velocity dispersion (typically more than 1000 km/sec) and, statistically, a more compact structure.

## 3. The Project

In 1986 we started a systematic survey of clusters of galaxies at intermediate and large redshift ( $0.15 < z < 0.6$ ). Previous contributions to this long-term project can be found in Buzzoni et al. (1988), Molinari et al. (1990), Molinari et al. (1992).

To date a homogeneous set of CCD observations in the Gunn  $g, r, i$  system has been collected mainly using the 3.6-m ESO telescope at La Silla equipped with EFOSC. About ten clusters

have been observed down to the limiting magnitude  $r \sim 24$ . Data reduction and systematic photometry in the fields have been performed using MIDAS utilities, and the implemented package INVENTORY (West and Kruszewski 1981). A parallel investigation including multi-object spectroscopy of selected relevant candidates in each field had also been carried out allowing to explore in more detail the absolute spectral energy distribution of the galaxies.

Although of the greatest importance, the spectroscopic approach cannot be widely pursued as it is largely time-consuming. Even fully exploiting the EFOSC MOS mode we need about 4-7 hours integration time to obtain spectra of acceptable signal-to-noise for objects fainter than 20th magnitude. For comparison, good photometry down to magnitude 24 can be achieved in about 1 hour total exposure time. Our analysis rests therefore basically on the multicolour photometry using spectral information as a check of our inferences.

Through comparison with evolutionary population synthesis models (Buzzoni 1988, 1989) we intend to study how consistently photometric properties (i.e. magnitudes and colours) of galaxies in clusters do evolve in a "regu-

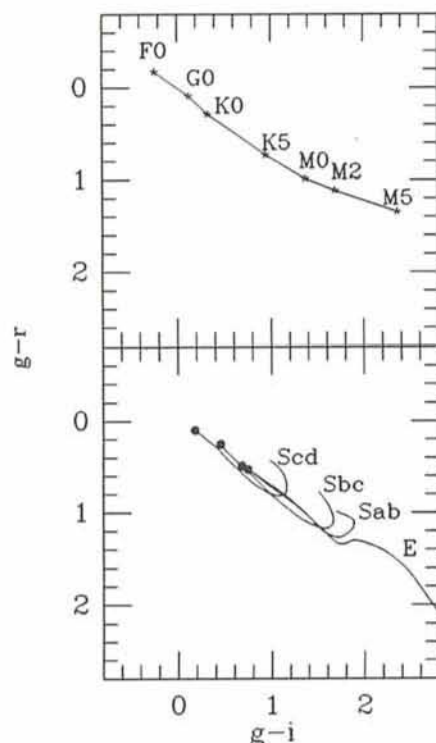


Figure 2: Two-colour diagram for the main-sequence stars (upper panel). In the lower panel the colour excursion for the different galaxy morphological types as a function of redshift (from  $z = 0$  to 1 in the sense of increasing  $g-i$ ) are shown with the zero-redshift points marked by filled dots (from Molinari et al. 1990).

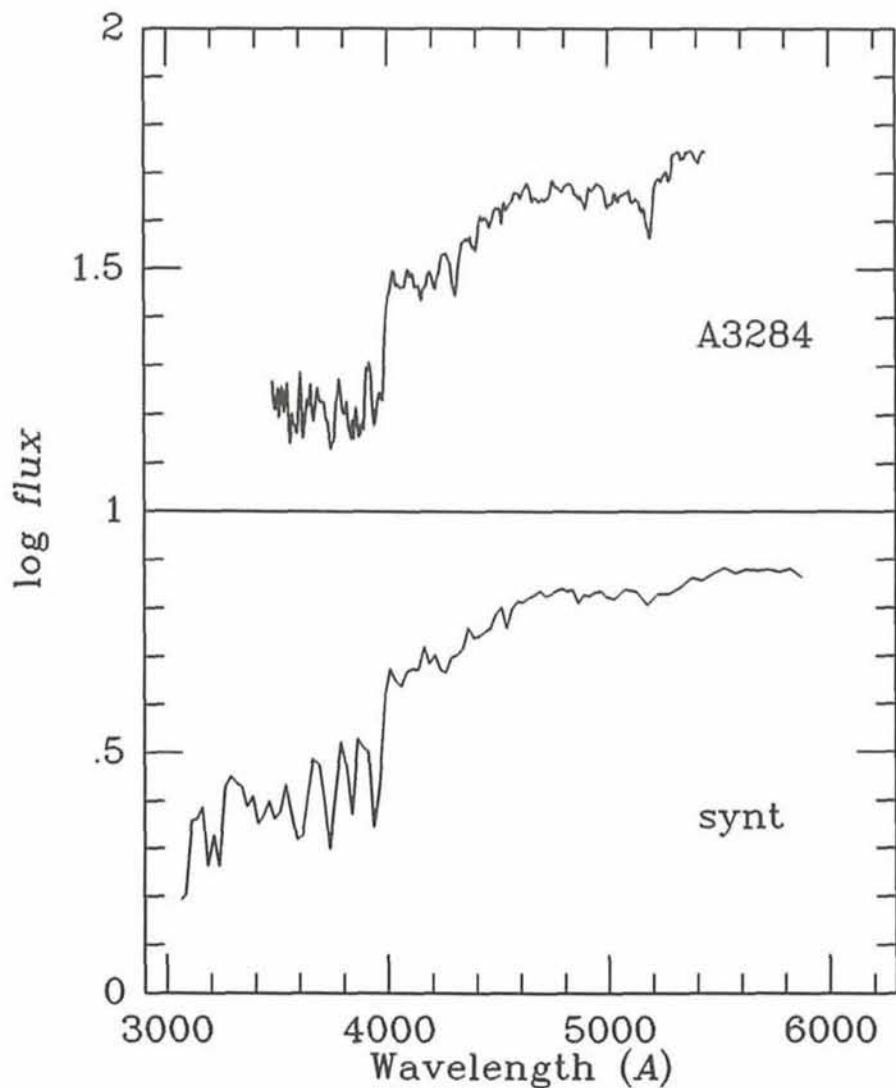


Figure 3: Observed and theoretical spectral distribution of elliptical galaxies. In the upper panel four spectra of red galaxies in the cluster A3284 have been coadded and reduced to restframe (six hours total exposure time with the ESO 3.6-m telescope + EFOSC, Grism B300 with a 230Å/mm dispersion). The lower panel shows for comparison an appropriate synthetic model for a 15 Gyr single burst stellar population (from Buzzoni 1989, his model No. 10 in Table 8).

lar" way following the prescription of stellar evolution. All those which deviate from the expectations will tell us something new, that is about events which have perturbed and/or accelerated the normal course of the evolution. This might be expected especially at high redshift.

#### 4. Galaxy Type and Colour Segregation

A 25 kpc linear size galaxy at redshift  $z$  in a  $q_0 = 0$  Universe is about  $1.8h(1+z)^2/[z(1+z/2)]$  arcsec across (where  $H_0 = 100h$  km/sec/Mpc). Its surface brightness dims as  $(1+z)^{-4}$  so that this makes very difficult or even impossible to estimate the morphology at high redshift. Beyond  $z \sim 0.2$  any direct morphological classification becomes unreliable even in deep CCD frames when taken under typical instrumental and

seeing conditions. That is why we must rely on colours to identify galaxy types.

A two-colour diagram could be used effectively to discriminate between late-type and early-type galaxies in distant clusters. Furthermore, combining it with a colour-magnitude diagram we can also discriminate between foreground and background objects (respectively too bright and too faint to be members of similar apparent colour). On the basis of accurate photometry we showed that redshift of distant clusters (up to  $z \sim 0.45$ ) can be inferred from apparent galactic colours within a 10% accuracy (Molinari et al. 1990).

In Figure 1 we show some relevant  $(g-r)/(g-i)$  diagrams for three clusters of our sample with  $z$  spanning between 0.15 and 0.50. In each panel the photometry of all objects in the fields is reported. Some striking features are worth of attention. (i) Both field stars and

galaxies spread along a diagonal strip in the diagram; (ii) the density along the strip is not constant and one clearly detects in each panel a clump of objects (encircled in the figure) moving to redder colours with increasing redshift; (iii) a tail of a few faint objects is always present redward the clump. Their apparent magnitude is correlated with colours, the reddest ones being also the faintest.

A full comprehension of the diagrams can be eased by comparing them with the two panels of Figure 2. In the first one we reported the locus expected for Galactic field stars of different spectral type while in the second panel we display the apparent colour excursion of galaxies of different morphological types with increasing redshift. It is now clear that the clump of objects observed in the colour-colour diagrams is originated by early-type galaxies at a redshift pertinent to that of the parent cluster.

Moreover, as a general rule we can note that foreground galaxies always lie blueward of the colour of the main clump due to the fact that E-galaxies are systematically the reddest objects within a given redshift. Accordingly, the faint tail of red objects with  $g-i > 2$  is mainly contributed by field galaxies in the background (at  $z > 0.5$ ) belonging to early types (spirals can never reach such colours as displayed in Figure 2). Also a few distant QSOs might be expected to lie in this zone (Irwin et al. 1991).

A complete support of the fact that galaxies in the main clump of the  $(g-r)/(g-i)$  diagram can be the true progenitors of present-day ellipticals comes from the analysis of the spectra as shown in Figure 3. Here, an averaged spectrum obtained by summing up four red galaxies in A3284 is compared with a synthetic model of a 15 Gyr burst stellar population taken from Buzzoni (1989, his model No. 10 in Table 8).

#### 5. What Contributes to the Blue Excess?

A more simple approach to the study of the cluster galaxy population rests also on the analysis of the single colour distribution like in Figure 4. In the figure we reported the  $g-i$  distribution observed for the clusters A3284. Considering all the objects available (thick line in the figure) one clearly recognizes the major bump due to the early-type component in the cluster population as previously discussed. A second peak appears to bluer colours ( $g-i \sim 0.5$ ) that we interpret as late-type galaxies. This group contains the excess blue galaxies claimed by Butcher and Oemler.

Following the canonical prescriptions (Butcher and Oemler 1984b) we were able to derive the fraction  $f_b$  of blue

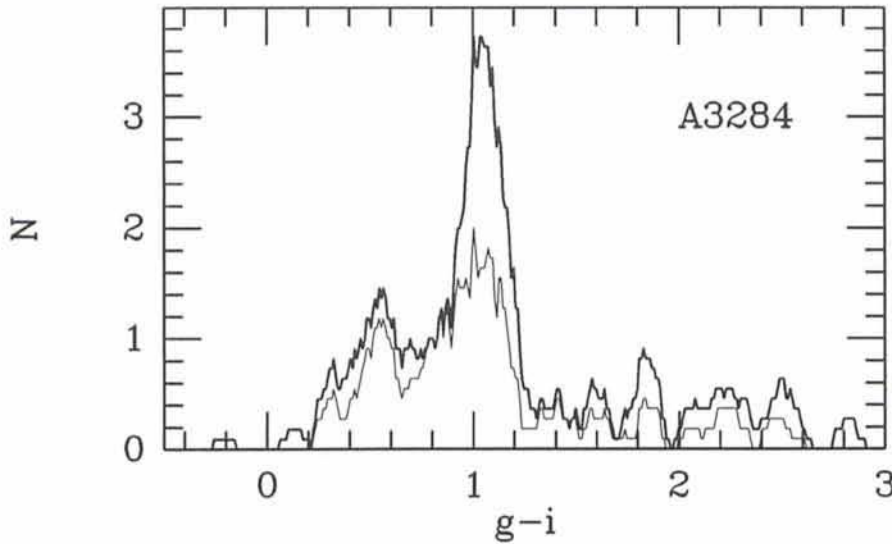


Figure 4: Histogram of the  $g-i$  colour distribution in the cluster A3284. The thick line represents the distribution of the whole sample of measured objects, while the thin line accounts for the subsample fainter than  $r = 21.5$ . The histogram is generated by a moving average with beam  $0.3 \text{ mag}$  and step  $0.01 \text{ mag}$ .

galaxies for this cluster and for some others in our sample. The results are summarized in Figure 5 where we compare consistently with the work by Newberry et al. (1988). Our data confirm the Butcher-Oemler effect, with the blue galaxies becoming an increasing fraction of the high- $z$  cluster population.

It is remarkable to note however that both on the basis of our photometric and spectroscopic observations collected to date we do not find any evident sign that the blue excess is due to an extensive presence of active or peculiar galaxies. The radial distribution of the galaxies in the blue bump in fact seems to closely match the trend observed by Whitmore and Gilmore (1991) for normal spirals in a large sample of low-redshift clusters. The question that arises is therefore whether we are observing somehow "active" blue elliptical galaxies or, more likely, a population of spiral-like galaxies.

A striking feature which seems to appear from the observations and could be worth further investigation is that blue galaxies in our sample tend to become relevant at the faint tail of the galaxy luminosity function. This is evident for example in Figure 4 where the thin line shows for A3284 the colour distribution of the objects fainter than  $r = 21.5$  ( $M_B > -17.5$  assuming  $H_0 = 50 \text{ km/sec/Mpc}$ ).

As this magnitude roughly coincides with the limit where dwarf and non-dwarf galaxies contribute at the same level to the luminosity function (Binggeli et al. 1988) we are not able to univocally identify the real nature of the blue excess. A more complete and deep database will allow us to discriminate

whether or not in the clusters at high redshift the population of dwarfs was more evident, and therefore favours or disfavors the hypothesis of a luminosity-dependent evolution, as the recent results dealing with the dwarf-galaxy nature of the blue excess in the field counts seem to suggest (Cowie et al., 1991).

#### References

Binggeli, B., Sandage, A. and Tamman, G.A. 1988, *Ann.Rev.Astr.Ap.*, **26**, 509.  
 Butcher, H. and Oemler, A. 1984a, *Nature*, **310**, 31.

Butcher, H. and Oemler, A. 1984b, *Ap.J.*, **285**, 426.  
 Buzzoni, A. 1988, *Erice Workshop, Towards Understanding Galaxies at Large Redshift*, eds. R.G. Kron and A. Renzini (Dordrecht: Kluwer) p. 61.  
 Buzzoni, A. 1989, *Ap.J.Suppl.*, **71**, 817.  
 Buzzoni, A. Molinari, E.C., Manousoyannaki, I. and Chincarini, G. 1988, *The Messenger*, **53**, 50.  
 Cappi, A., Chincarini, G., Conconi, P. and Vettolani, G. 1989, *Astr.Ap.*, **223**, 1.  
 Coleman, G.D., Wu, C. and Weedman, D.W. 1980, *Ap.J.Suppl.*, **43**, 393.  
 Cowie, L.L., Songaila, A. and Mu, E.M. 1991, *Nature*, **354**, 460.  
 Dressler, A. 1980, *Ap.J.*, **236**, 351.  
 Dressler, A. and Gunn, J.E. 1982, *Ap.J.*, **263**, 533.  
 Dressler, A. and Gunn, J.E. 1983, *Ap.J.*, **270**, 7.  
 Irwin, M.J., McMahon, R.G. and Hazard, C. 1991, *The Space Distribution of Quasars*, ed. D. Crampton, Astr. Soc. of the Pac. Conf. Ser., vol. 21, p. 117.  
 Koo, D.C. 1988, *Erice Workshop, Towards Understanding Galaxies at Large Redshift*, eds. R.G. Kron and A. Renzini (Dordrecht: Kluwer) p. 275.  
 Luppino, G.A., Cooke, B.A., McHardy, I.M. and Ricker, G.R. 1991, *Astr.J.*, **102**, 1.  
 Molinari, E., Buzzoni, A. and Chincarini, G. 1990, *M.N.R.A.S.*, **246**, 576.  
 Molinari, E., Pedrana, M.D., Banzi, M., Buzzoni, A. and Chincarini, G. 1992, *Proceedings of the IAU Symp. No. 149 "The Stellar Populations of Galaxies"*, eds. B. Barbuy and A. Renzini (Dordrecht: Kluwer) p. 460.  
 Newberry, M.V., Kirshner, R.P. and Boroson, T.A. 1988, *Ap.J.*, **335**, 629.  
 Thompson, L.A. 1988, *Ap.J.*, **324**, 112.  
 West, R.M. and Kruszewski, A. 1981, *Irish Astr.J.*, **15**, 25.  
 Whitmore, B.C. and Gilmore, D.M. 1991, *Ap.J.*, **367**, 64.

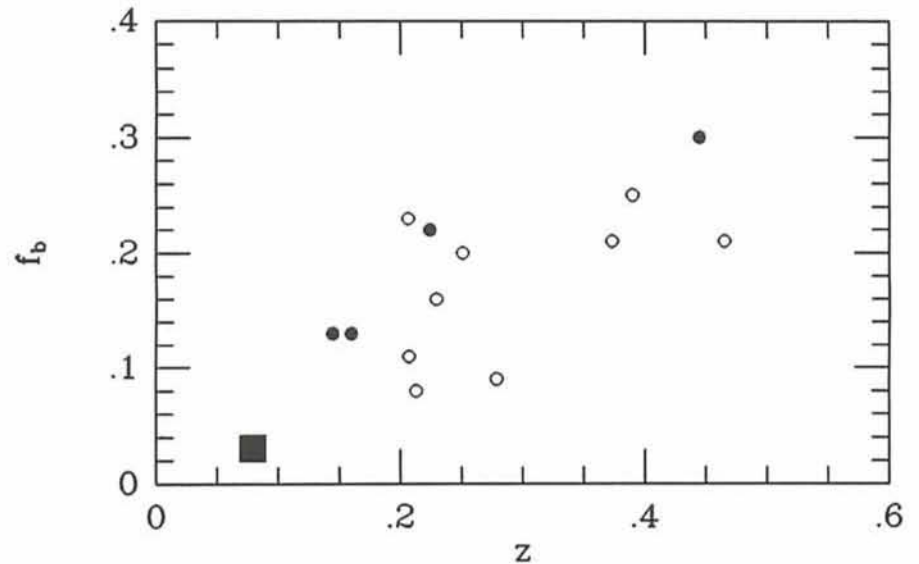


Figure 5: Diagram showing the fraction of blue galaxies  $f_b$ . Open dots are taken from Newberry et al. (1988, their Fig. 2). The filled square bottom left is the mean estimate for 8 low-redshift clusters (up to  $z = 0.08$ ) from Butcher and Oemler (1984b). Filled dots are our data and refer to the clusters A3284, A3305, A1942 and 2158+0351 in order of increasing redshift.